ARTICLE

NMR spectroscopic detection of chirality and enantiopurity in referenced systems without formation of diastereomers

Jan Labuta[1], Shinsuke Ishihara[1], Tomáš Šikorský[2], Zdeněk Futera[3,†], Atsuomi Shundo[1,†], Lenka Hanyková[4], Jaroslav V. Burda[3], Katsuhiko Ariga[1,5] & Jonathan P. Hill[1,5]

Enantiomeric excess of chiral compounds is a key parameter that determines their activity or therapeutic action. The current paradigm for rapid measurement of enantiomeric excess using NMR is based on the formation of diastereomeric complexes between the chiral analyte and a chiral resolving agent, leading to (at least) two species with no symmetry relationship. Here we report an effective method of enantiomeric excess determination using a symmetrical achiral molecule as the resolving agent, which is based on the complexation with analyte (in the fast exchange regime) without the formation of diastereomers. The use of N,N'-disubstituted oxoporphyrinogen as the resolving agent makes this novel method extremely versatile, and appropriate for various chiral analytes including carboxylic acids, esters, alcohols and protected amino acids using the same achiral molecule. The model of sensing mechanism exhibits a fundamental linear response between enantiomeric excess and the observed magnitude of induced chemical shift non-equivalence in the ^{1}H NMR spectra.

[1] International Center for Materials Nanoarchitectonics (MANA), National Institute for Materials Science (NIMS), 1-1 Namiki, Tsukuba, Ibaraki 305-0044, Japan. [2] CEITEC—Central European Institute of Technology, Masaryk University, CZ-62500 Brno, Czech Republic. [3] Charles University in Prague, Faculty of Mathematics and Physics, Department of Chemical Physics and Optics, Ke Karlovu 3, 121 16 Prague 2, Czech Republic. [4] Charles University in Prague, Faculty of Mathematics and Physics, Department of Macromolecular Physics, V Holešovičkách 2, 180 00 Prague 8, Czech Republic. [5] Japan Science and Technology Agency (JST), Core Research for Evolutional Science and Technology (CREST), 1-1 Namiki, Tsukuba, Ibaraki 305-0044, Japan. † Present addresses: Keio University, 3-14-1 Hiyoshi, Kohoku-ku, Yokohama 223-8522, Japan (Z.F.); Department of Applied Chemistry, Faculty of Engineering, Kyushu University, 744 Motooka, Nishi-ku, Fukuoka 819-0395, Japan (A.S.). Correspondence and requests for materials should be addressed to J.H. (email: Jonathan.Hill@nims.go.jp).

Chirality plays a key role in many biological events but is also important in the development of new pharmaceuticals[1], for control of organic asymmetric reactions[2], chiral catalysis[3,4] and in several aspects of supramolecular science[5–10]. Therefore, the detection of chirality, including analysis of chiral purity and interactions between chiral species, is an intensive area of research. Various procedures for determining analyte chirality have been proposed and those of note are based on optical (for example ultraviolet/visible spectrophotometry (uv/Vis)[11–13], circular dichroism (CD)[14,15], fluorescence[16–19]) and electrochemical[20] methods involving a synthetic chiral host as a chirality detector. However, the use of an achiral host as a detector has only seldom been achieved, that is, through the formation of ternary diastereomeric complexes between chiral substrate molecules and achiral host[21] or by the observation of exciton-coupled CD effects in porphyrin tweezer molecules where helicity is induced by complexation with a chiral guest[22–25].

Over several decades NMR spectroscopic methods, which depend on a chiral auxiliary such as chiral derivatization agent[26–28], chiral lanthanide shift reagents[26,29] and chiral solvating agents (CSA)[27–30] have been extensively studied. NMR discrimination methods that do not use an auxiliary have also been developed[31–33] although they are considered unusual as self-association between chiral analytes is required in the formation of diastereomeric dimers. Use of an achiral auxiliary in conjunction with ^{31}P NMR spectroscopy has also been reported[34]. However, in that case an achiral derivatization agent was used as a platform for covalent coupling of two chiral analyte molecules resulting in diastereomer formation and three well-separated NMR resonances could be observed. We have previously reported a method that facilitates the latter concept by using a solvating agent where a host–guest complex (formed via non-covalent interaction) between an achiral host and two chiral guests is formed[35,36]. In that case, formation of two rapidly exchanging diastereomers occurs and resulting NMR spectra show two distinct resonances whose separation reflects proportionally the enantiomeric excess of the chiral guest. Chiral liquid crystals[37–39] have been used as anisotropic solvents to differentiate enantiotopic directions of prochiral analyte molecules without diastereomer formation although in that case the analyte resonances are observed (however, if chiral analyte molecules are dissolved in chiral liquid crystals diastereomeric pairs are formed).

Based on these examples it seems that NMR, as an intrinsically achiral method, lacks the capability to sense chirality or enantiomeric excess (e.e.) in the absence of a chiral auxiliary, or of self-association of chiral analytes, or without formation of at least 1:2 complexes of achiral agent:chiral analyte. In all cases, formation of diastereomeric species occurs in solution and utilization of NMR in conjunction with an achiral reagent in non-diastereomeric binding mode as a probe of enantiopurity remains challenging. Such processes where 'achiral' can sense 'chiral' might have connotations for enantioselective amplification, as well as for the origin of homochirality in living organisms[40].

In this work, we introduce a ^{1}H NMR versatile prochiral solvating agent (pro-CSA) for determination of chirality and e.e. which does not rely on formation of diastereomeric pairing between prochiral host and chiral analyte; rather, a pair of enantiomeric complexes are formed. Detection of information about a chirality/e.e. without employing formation of diastereomers has not to our knowledge been reported and is an unusual and intriguing aspect of our pro-CSA host. The pro-CSA host molecule contains appropriate prochiral CH reporter groups, which facilitate e.e. discrimination. The nature of chirality detection and e.e. sensing are rationalized in terms of 1:1 host–guest complexation between pro-CSA molecule, represented by the N,N′-disubstituted oxoporphyrinogen host molecule **H**, and

various chiral guest molecules **G***, including carboxylic acids and esters, amino acid esters, N-protected amino acids, and some terpenoids such as menthol and camphor. Experimental and theoretical methods (NMR, uv/Vis, CD, quantum mechanical (QM) calculations and classical molecular dynamics (MD) simulations) are used to elucidate the chirality and/or e.e. sensing properties of the system presented here.

Results

Symmetry and origin of chemical shift non-equivalence. The e.e. discrimination method presented here relies fundamentally on the concept of prochirality[41], defined as 'the geometric property of an achiral object (or spatial arrangement of points or atoms) which is capable of becoming chiral in a single desymmetrization step'[42]. It is known that when a prochiral compound (for example, an achiral primary carboxylic acid $Ph(CH_2)CO_2H$) is placed in a chiral environment (for example, (+)-(1R,2R)-1,2-diphenylethane-1,2-diamine) forming an acid-amine complex, the enantiotopic (prochiral) methylene hydrogens of the acid exhibit chemical shift non-equivalency and thus are rendered diastereotopic[43,44]. The pro-CSA, **H**, presented here contains enantiotopic CH reporter groups as shown in Fig. 1a. When an enantiopure chiral guest (Fig. 1b) is added to a solution of host molecule **H** symmetrical splitting (sometimes with an associated up- or downfield shift) of the resonance due to the reporter groups can be observed (Fig. 1c). **H** complexes with a chiral guest by hydrogen bonding through pyrrolic NH groups located at its centre resulting in downfield shift of the NH proton resonance (Fig. 1c). Taking into account the host's saddle shape and the relative rigidity of its macrocycle, the distance of the available CH reporter groups from the binding site has an important role. Each CH group exhibits different sensitivity (that is, magnitude of non-equivalency) to different chiral guests (Fig. 1c). As **H** has four such groups of practical use at different spatial positions (accessibility) and distances from the binding site there is a good chance that any chiral guest with affinity to bind to **H** will cause non-equivalency in selected or all of the CH reporter groups.

At this point, the origin of chemical shift non-equivalency of CH reporter groups can be elucidated in terms of the symmetry of **H** and disruption thereof upon interaction with a chiral guest. The term 'prochirality' is frequently used to describe systems where replacement of a single ligand leads to a stereogenic centre[45]. The equivalent of this in non-covalently interacting systems would be the formation of diastereotopic nuclei from initially enantiotopic nuclei due to an external factor as illustrated above in the case of acid-amine complexes where the methylene carbon of $Ph(CH_2)CO_2H$ can be considered a 'stereogenic centre'. However, the CH reporter groups of **H** do not posses the property that any of its carbon atoms could be converted to a 'stereogenic centre'. For simplicity let us consider the complexation of **H** with **1a** where the CH reporter groups of interest are at the β positions of the N-alkylated pyrrole group (β-H; Fig. 2a,b). In the structure of **H**, two prochiral planes[44] are present (Fig. 2a). More specifically, two onefold improper rotations S_1 (= mirror planes σ_d), which are identical with prochiral planes, can be identified. These mirror planes make group A and B of β-H interconvertible and hence enantiotopic (magnetically equivalent with isochronous NMR resonances)[44,46].

Note that **H** also possesses a proper symmetry axis C_2, which might suggest that groups A and B are homotopic hence isochronous even in a chiral environment. However, groups A and B (as defined in Fig. 2a) cannot be interconverted using C_2. Therefore, in general, β-H nuclei are required to be identified as groups A and B so that they are interconvertible by improper rotation S_n (including plane σ or centre of symmetry i) and not
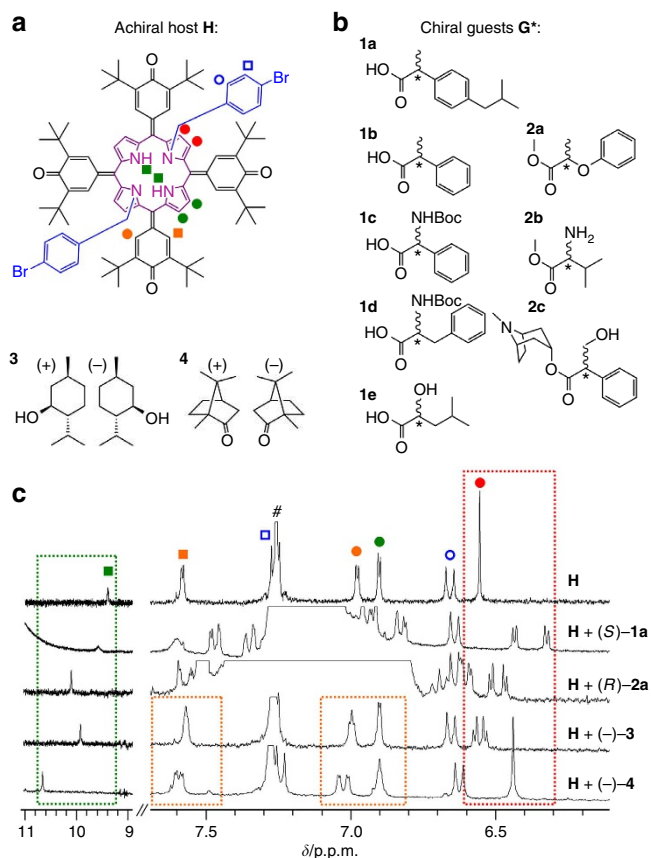
Figure 1 | Structures of host and guests and their NMR properties.
(**a**) Structure of achiral host N_{21},N_{23}-*bis*(4-bromobenzyl)-5,10,15,20-*tetrakis*
(3,5-di-*t*-butyl-4-oxocyclohexadien-2,5-ylidene)porphyrinogen, **H**. Symbols
denote the peak assignments in all ^{1}H NMR spectra in this study.
(**b**) Structure of chiral guests used: ibuprofen **1a**, 2-phenylpropionic acid **1b**,
N-boc-2-phenylglycine **1c**, N-boc-phenylalanine **1d**, leucic acid **1e**, 2-
phenoxypropionic acid methyl ester **2a**, valine methyl ester **2b**, atropine
(hyoscyamine) **2c**, menthol **3** and camphor **4** (boc = *tert*-butoxycarbonyl).
(**c**) Typical ^{1}H NMR spectra of chloroform-*d* solution of neat **H** (ca. 0.7 mM)
and **H** (ca. 0.7 mM) with ca. 400 equiv. of selected chiral guests. Key:
Green square (pyrrolic NH); enantiotopic CH reporter groups: orange
square and circle (hemiquinonoid *ortho*-H), green circle (N-H pyrrolic β-H)
and red circle (N-alkylated pyrrolic β-H). Hash symbol denotes residual
chloroform (CHCl_3). Full **H** spectrum assignment is provided in
Supplementary Figs S1–S3.

by operation of proper symmetry axes C_n.[44] In that case, groups
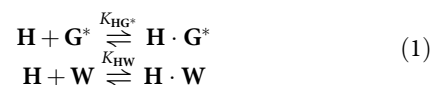A and B are enantiotopic.

The presence of a chiral guest leads to magnetic non-
equivalence of group A and B as it affects each group of protons
in a different manner as can be illustrated (from MD simulations)
by the preference of certain orientations of guest occupation (that
is, conformations) over others as shown in Fig. 2c,d. A chiral
environment breaks mirror symmetry and the initially enantio-
topic groups A and B become diastereotopic with distinguishable
anisochronous NMR resonances (Fig. 2b). Note that group A and
B are contained in the same molecule so that no actual
diastereomers are present. This is also the reason why at any
arbitrary e.e. the split peaks have the identical intensities. The
second-order quartet (which exhibits roofing) appears as a
consequence of the close structural connection between H_A and
H_B protons, which have a vicinal scalar [3]*J*-coupling constant.
From QM calculations it can be identified which group of protons
will experience upfield or downfield shifts (see Supplementary

Fig. S4). QM results for the **H**·(*R*)-**1a** complex reveal that group
A is shifted relatively upfield compared with group B and vice
versa due to symmetry of the complex **H**·(*S*)–**1a**.

NMR spectral properties and binding model. Hydrogen bond-
ing between **H** and chiral guest appears to be weak so that a
relatively high concentration of chiral guest is required to obtain
well-resolved spectral lines (Fig. 1c). Interestingly, if the con-
centration of chiral guest is kept constant and e.e. is varied then
the magnitude of splitting $\Delta\delta$ of spectral lines varies linearly with
e.e. (Fig. 3a–d, for other guests see Supplementary Figs S5–S14).
The linear dependence of $\Delta\delta$ on e.e. is a fundamental property of
pro-CSA molecules as will be shown later. When determining the
true resonance frequency of the N-alkylated pyrrolic β-H, N-H
pyrrolic β-H and hemiquinonoid *ortho*-H spin systems it must be
taken into consideration that these spins are second-order
strongly coupled systems, and the fitting procedure should be
carried out with appropriate care (see ^{1}H NMR spectra fitting in
Supplementary Methods). The characteristic roofed shape of the
split N-alkylated pyrrolic β-H resonances and the cross-peaks
between them in ^{1}H–^{1}H COSY spectrum (Fig. 3e) clearly indi-
cates that both peaks originate from the same host molecule.
Similar cross-peaks were observed in N-H pyrrolic β-H and
hemiquinonoid *ortho*-H in, for example, **H**·(−)−**4** complex (see
^{1}H NMR spectra fitting in Supplementary Methods). As e.e. tends
towards 0% (that is, racemic mixture), a single set of sharp well-
resolved resonances remain. At 0% e.e. these converge to a
centred singlet for **H**·**1a**, **H**·**2a** and a doublet for **H**·**4** (Fig 3a–c).
The lack (at 0% e.e.) of two sets of peaks, corresponding to stable
complexes of **H**·(*R*)-enantiomer and **H**·(*S*)-enantiomer, indi-
cates fast exchange of chiral guests at the host's binding site.

The above-mentioned features helped us to elucidate the origin
of the linear relationship between magnitude of splitting $\Delta\delta$ and
e.e., as well as a model of the host–guest binding mechanism. The
mechanism of binding should be considered as competitive
involving binding of water molecules **W** and the chiral guest **G**[*]
to the host molecule **H**, as titration of a chloroform solution of **H**
with **W** yields a not insignificant response (and high binding
constant) to traces of water (Fig. 4a, for ^{1}H NMR spectra see
Supplementary Fig. S15)[47]. Moreover, water is ubiquitous and is
difficult to remove from chloroform, which also explains why a
relatively high concentration of **G**[*] is required to obtain well-
resolved split NMR spectra. Some examples of titrations of **H** with
3 are shown in Fig. 4b–e (for other guests and other types of
titrations see Supplementary Figs S16–S25). For the two types of
titration shown it can be observed that the chemical shift of
pyrrolic NH resonance (δ_{NH}) increases monotonically while
splitting of N-substituted pyrrolic β-H ($\Delta\delta$) does not necessarily
increase monotonically (compare Fig. 4b,c). These observations
suggest that the NH group reflects only the overall binding of
guests (**G**[*] or **W**) while the pyrrolic β-H protons are sensitive not
only to overall binding but also to the nature of chiral guest and its
e.e. Therefore, binding isotherms are required to be constructed
(and fitted) simultaneously for both δ_{NH} and $\Delta\delta$, as they each
partially express the same characteristic (binding strength).

Binding isotherms for δ_{NH} and $\Delta\delta$ can be constructed based on
a 1:1 host:ligand (where ligand can be chiral guest **G**[*] or water **W**)
competitive binding model (Fig. 5a) as described by the
equilibrium equations 1.

$$\mathbf{H} + \mathbf{G}^* \underset{K_{HG^*}}{\overset{K_{HG^*}}{\rightleftharpoons}} \mathbf{H} \cdot \mathbf{G}^*$$
$$\mathbf{H} + \mathbf{W} \underset{K_{HW}}{\overset{K_{HW}}{\rightleftharpoons}} \mathbf{H} \cdot \mathbf{W}$$
(1)

where K_{HG^*} and K_{HW} are the equilibrium binding constants of
formation of **H**·**G**[*] and **H**·**W** complexes, respectively. In the
derivation of binding isotherms we assume fast exchange between
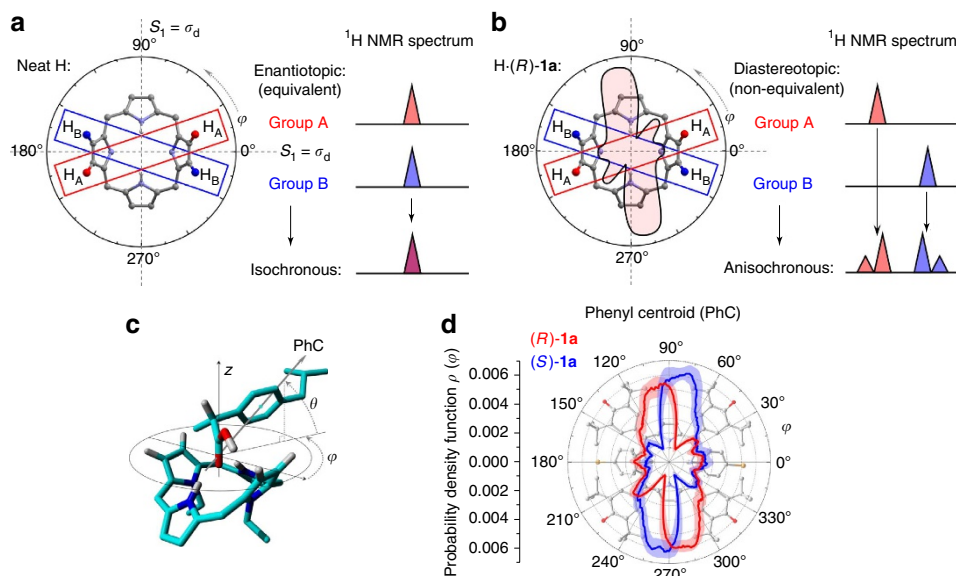
Figure 2 | Effect of guest complexation on symmetry of the host molecule. (**a**) Scheme of symmetry of host molecule and corresponding shape of NMR spectra. Dashed lines denote axes of S_1 symmetry elements (mirror planes) also identical to prochiral planes. (**b**) Disruption of host's symmetry upon complexation with chiral guest and resulting splitting of NMR spectral pattern. (**c**) Schematic plot of reference system connected with host and orientation of guest within it using φ and θ coordinates used in the MD simulations. (**d**) Plot of probability density function $\rho(\varphi)$ as obtained from MD simulations (for $\mathbf{H} \cdot (R)$-**1a** and $\mathbf{H} \cdot (S)$-**1a** complexes) for phenyl centroid (PhC). Solid red or blue lines show average $\rho(\varphi)$ over 5°. Light red or blue background denotes standard variance of $\rho(\varphi)$. Supplementary Movie 1 depicts MD of the spontaneous release of (S)-**1a** from the binding site with subsequent binding of (R)-**1a** (video length in real time is 4.4 ns).
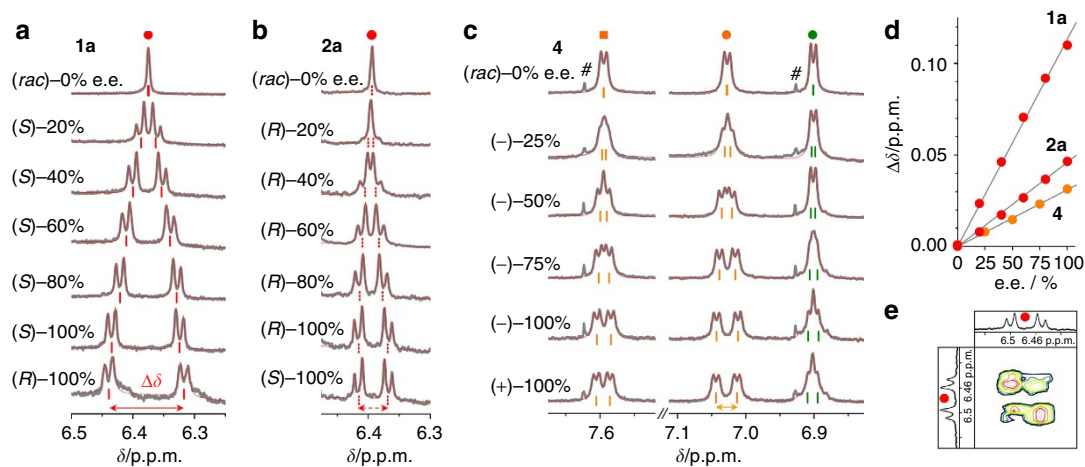

Figure 3 | ¹H NMR data showing dependency of chemical shift non-equivalency on e.e. (**a**,**b**,**c**) Spectra of **H** (0.68 mM, chloroform-*d*) in the presence of various e.e. of **1a** (460 equiv.), **2a** (370 equiv.) and **4** (490 equiv.) at 25 °C, respectively. Hash symbol denotes carbon-13 satellite from chloroform-*d* solvent. All spectra were fitted (grey = original spectrum, red = fit) and true resonance frequencies as obtained by fit are indicated by lines under each spectrum. Spectra for **1a** and **2a** were taken as AB second-order strongly coupled quartet. Left part of spectrum (orange circle and square) for guest **4** was fitted as two independent EF and E'F' second-order spin systems and right part of spectrum (green circle) as CDX strongly coupled quartet of doublets (for details see ¹H NMR spectra fitting in Supplementary Methods). (**d**) Plot of dependency of $\Delta\delta$ on the e.e. value of host's splitted resonance (denoted by arrows in **a**–**c**) showing linear relationship (for all $R^2 > 0.997$). (**e**) Homonuclear ¹H–¹H COSY spectrum of N-alkylated pyrrolic β-H resonances of **H** (1.42 mM, chloroform-*d*) with (S)-**1a** (200 equiv.) at 25 °C.

the three states of host $\mathbf{H} \cdot \mathbf{G}^*$, $\mathbf{H}$ and $\mathbf{H} \cdot \mathbf{W}$ (Fig. 5a) and that binding of (R)- or (S)-enantiomer to the host is statistical due to the symmetry of $\mathbf{H}$. Then δ_{NH} and $\Delta\delta$ can be expressed in the form of equations 2 and 3, respectively (for the full derivation see Methods).

$$\delta_{NH} = p_{HG^*} \times {}^{NH}\delta_{HG^*} + p_H \times {}^{NH}\delta_H + p_{HW} \times {}^{NH}\delta_{HW} \quad (2)$$

$$\Delta\delta = \Delta\delta_{max} \times \text{e.e.} \times p_{HG^*} \quad (3)$$

where p_{HG^*}, p_{HW} and p_H (as defined by equation 5 in Methods) are populations of all the host forms, $\mathbf{H}$ bound to $\mathbf{G}^*$ or $\mathbf{W}$ and free $\mathbf{H}$, respectively. Simultaneous fitting of the binding isotherms, δ_{NH} and $\Delta\delta$, with experimental data yields characteristic values, in particular K_{HG^*}, $\Delta\delta_{max}$ and ${}^{NH}\delta_{HG^*}$ (Table 1), for each pair of host and chiral guest. These values reveal that $\Delta\delta_{max}$ is independent of K_{HG^*} and seems to be strongly related to the dynamic structural conformation of each host–guest pair. The value of $\Delta\delta_{max}$ (or $\Delta\delta$ at particular concentration) for different
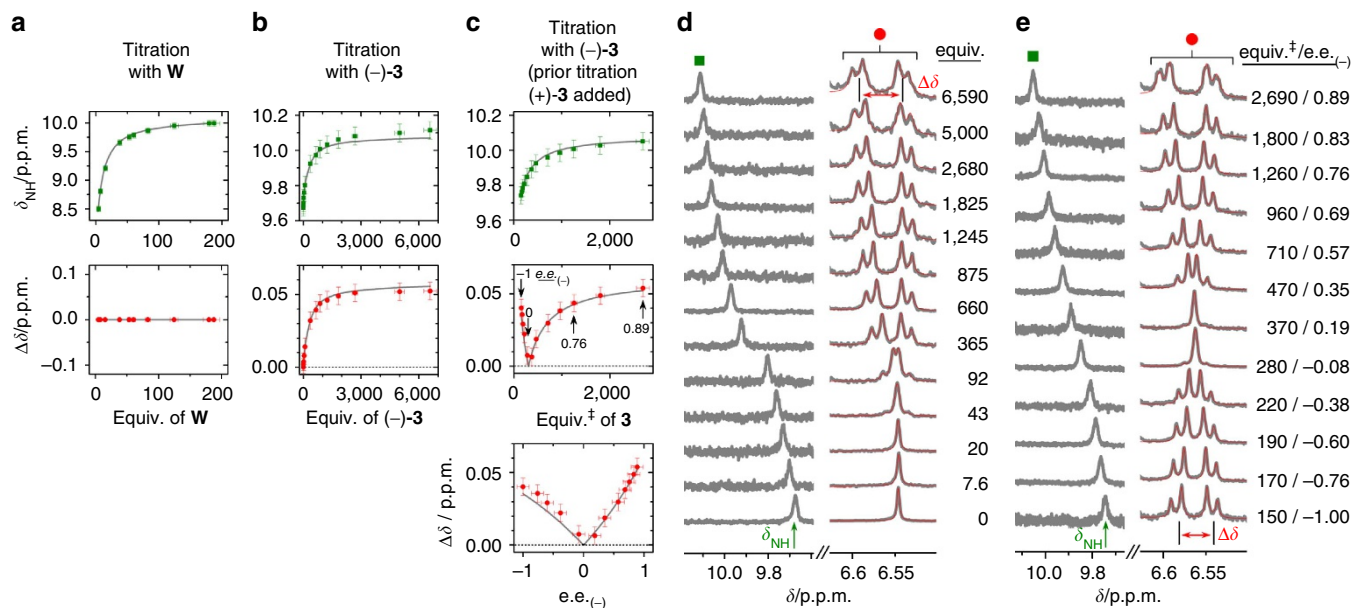
Figure 4 | ^{1}H NMR titration experiments supporting the competitive binding model. (**a**) Titration of **H** (0.41 mM, chloroform-*d*) with water **W** at 25 °C. (**b**) Titration of **H** (0.65 mM, chloroform-*d*) with (−)−**3** at 25 °C. (**c**) Titration of **H** (0.74 mM, chloroform-*d*) with (−)−**3** at 25 °C. Before titration (with (−)−**3**) 150 equiv. of (+)−**3** was added to the solution. Bottom panel shows dependency of $\Delta\delta$ on e.e. during the titration. Grey curves were fitted according to a competitive binding model (see Fig. 5) using isotherms expressed in equations 2 and 3. During titrations chiral guest and water concentrations were evaluated although water concentration did not vary significantly from initial value during titration. For binding constants and other parameters see Table 1. (**d,e**) Spectra taken during titration shown in **b,c**, respectively (grey = original spectrum, red = fit). Double dagger (‡) in **c,e** denotes combined concentration (in equiv.) of both enantiomers.
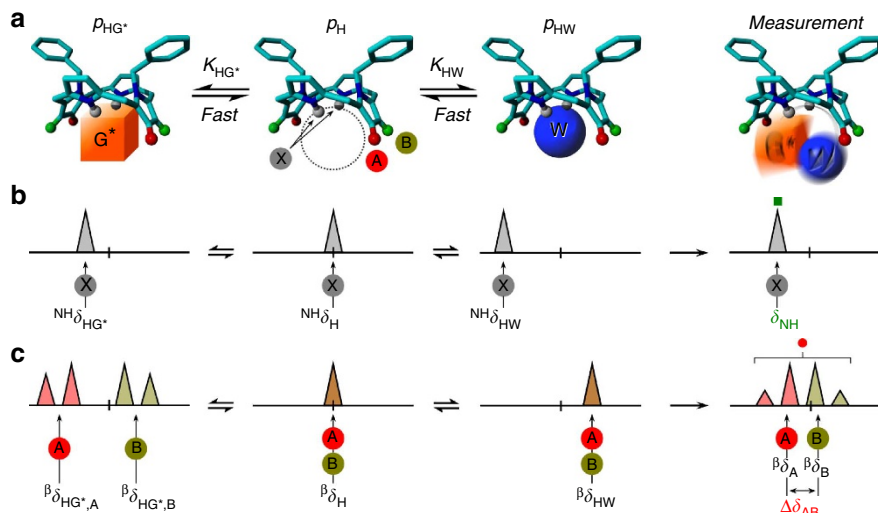
Figure 5 | Competitive binding model and its schematic ^{1}H NMR spectral manifestation. (**a**) Partial (*meso*-substituents removed) structural model of host, **H**, showing its three forms and (at right) an image illustrating the situation in solution. Equilibrium binding constants and populations are indicated. Protons of special interest (H_A, H_B and H_X) are also highlighted. (**b**) Schematic description of pyrrolic NH resonance (H_X) behaviour. (**c**) Schematic description of N-alkylated pyrrolic β-H resonances (H_A and H_B). Arrows indicate the true resonance frequency of spectral patterns.

chiral guests is, in general, not predictable (only rough estimations using density functional theory can be obtained) and without having a sample of pure enantiomer of analyte (or its known e.e. form) in hand it cannot be determined. Thus, construction of a linear calibration curve as seen in Fig. 3d seems to be a limiting factor for all pro-CSA.

The case of the **H** · (*R*)−**1a** complex was examined in detail using density functional theory (DFT) methods. Three possible conformations of host–guest complexes (Supplementary Data 1–3) and chemical shifts of N-alkylated pyrrolic β-H (for predicted

value of $\Delta\delta_{max}$ see Table 1) were calculated (see Supplementary Fig. S4). From data contained in Table 1 it can be seen that all the chiral guests studied have a low equilibrium binding constant so that direct confirmation of 1:1 binding stoichiometry using Job's plot is not feasible[48] as variation in δ_{NH} and $\Delta\delta$ was virtually unobservable when construction of a Job's plot was attempted. However, a competitive 1:1 binding model is supported by the fact that all titration experiments for various chiral guests, QM calculations and MD simulations show good agreement with the suggested model.

Guest	K_{HG^*}/M^{-1}	$\Delta\delta_{max}/p.p.m.^{\$}$	$^{NH}\delta_{HG^*}/p.p.m.$
1a	13 (± 3)	0.22 (± 0.02)	9.86 (± 0.05)
1a (calc.)†	—	0.30 ‡	11.02
1b	9 (± 3)	0.08 (± 0.02)	10.19 (± 0.25)
1c	9 (± 3)	0.07 (± 0.02)	10.70 (± 0.30)
1d	23 (± 8)	0.03 (± 0.01)	9.94 (± 0.10)
1e	42 (± 10)	0.03 (± 0.02)	10.70 (± 0.30)
2a	21 (± 4)	0.12 (± 0.02)	10.57 (± 0.05)
2b	12 (± 3)	0.025 (± 0.004)	10.79 (± 0.05)
2c	1.5 (± 0.4)	0.20 (± 0.04)	10.72 (± 0.27)
3	32 (± 8)	0.06 (± 0.02)	10.08 (± 0.05)
4	160 (± 25)	0.035 (± 0.005)§	10.79 (± 0.05)
W	240 (± 35)‖	0.00	10.09 (± 0.03)¶

Table 1 | Characteristic values for binding constants and isotherms.

Characteristic values of K_{HG^*}, $\Delta\delta_{max}$ and $^{NH}\delta_{HG^*}$ of the guests when complexed with host molecule **H** in chloroform-*d* at 25 °C for the competitive binding model.
$\$$Determined from splitting of N-alkylated pyrrolic β-H.
†Determined from DFT calculations.
‡Populations averaged value over all three conformations and over all four N-alkylated pyrrolic β-H shifts (see Supplementary Fig. S4).
§Determined from hemiquinonoid *ortho*-H resonances at 7.03 p.p.m.
‖The value refers to K_{HW}.
¶The value refers to $^{NH}\delta_{HW}$. The chemical shift of pyrrolic NH resonance of free host is $^{NH}\delta_H = 7.86$ (± 0.40) p.p.m. and 7.96 p.p.m. as determined from experimental data fitting and DFT calculations, respectively.

Equation 3 has some interesting consequences. It indicates a linear dependence on e.e., as well as on population of the $\mathbf{H \cdot G^*}$ complex. The apparent universal linearity of the $\Delta\delta$/e.e. plots indicates in turn that a calibration curve can always be constructed from a single measured point obtained from a sample of enantiopure analyte or a sample of independently measured e.e. (considering that a second point required for construction of a calibration curve has zero chemical shift non-equivalence $\Delta\delta = 0$ for the racemate where e.e. $= 0$). Also, the value of $\Delta\delta$ can be obtained by measurement only as a non-negative value, hence, only the absolute value of e.e. can be determined and enantiomeric identity remains unknown (for example, measurement gives e.e. $= 80\%$ but the excess enantiomeric form is not known). This principal indistinguishableness originates from the symmetry between enantiomeric complexes $\mathbf{H \cdot}(R)\text{-}\mathbf{G^*}$ and $\mathbf{H \cdot}(S)\text{-}\mathbf{G^*}$ and is present for all pro-CSA. It can be overcome only when a small amount of known enantiomer of guest is added. $\Delta\delta$ is either increased when the same enantiomer (as that in excess in solution) is added or decreased when the other enantiomer is added[36] (an example can be seen in Fig. 4b,d compared with Fig. 4c,e).

In order to investigate the transfer of chiral information from guest to host molecule the uv/Vis and CD spectra were recorded for most of the $\mathbf{H \cdot G^*}$ pairs (Supplementary Figs S26–S32). However, CD signal induced in the structure of $\mathbf{H}$ upon binding of $\mathbf{G^*}$ is very weak (compared with other systems for example, Mizuno *et al.*[14]) and can be detected only when large quantities of $\mathbf{G^*}$ are added to solution. This is due to the rigidity of the host's macrocyclic structure.

Temperature effects on the efficiency of e.e. sensing were explored using variable temperature (VT) ^{1}H NMR measurements (Supplementary Fig. S33). It can be seen that chemical shift non-equivalency $\Delta\delta$ is decreasing with decreasing temperature. This behaviour is rather unusual since the opposite (increasing chemical shift non-equivalency) should be observed with decreasing temperature. However, this is a consequence of the competitive binding model where at depressed temperature water binds to the host more strongly than the chiral guest leading to a decrease of overall $\Delta\delta$ value (which is reflected in equation 3 as a decrease of population of $\mathbf{H \cdot G^*}$ complex p_{HG^*}). VT-^{1}H NMR measurements also show that ambient temperature is optimal for e.e. analysis as it gives $\Delta\delta$ close to the maximum values, which is practical from the point-of-view of applications.

Discussion

Conventional CSA and the pro-CSA sensing method presented here have different characteristics. When a conventional diastereomer-forming reagent, for example a CSA, is used two separate resonances for each enantiomer appear although they cannot be unambiguously assigned to a particular enantiomer. Additional molecular modelling or chiroptical methods (for example, CD) are required to assign enantiomer identity. However, the value of e.e. can be obtained by integration of separate resonances without having an authentic sample of analyte in advance. The non-diastereomeric sensing mechanism of pro-CSA differs conceptually from but is complementary to the existing conventional methods.

From the point of practicality and potential use, the pro-CSA $\mathbf{H}$ presented here offers some noteworthy properties. First, when e.e. of the same analyte is required to be determined repetitively (for example, as in chemicals or pharmaceuticals industries) a calibration curve using pure enantiomers can be constructed once, which facilitates subsequent rapid analyses of e.e. by using a simple protocol. In this way, particular host–guest pairs would possess characteristic values of $\Delta\delta$ under the specified conditions. This method is then also appropriate for use in various enantioenrichment (Soai reaction[49]) studies as a rapid probe of e.e. values. In fact, in any case where initial purification (by chiral high-performance liquid chromatography or crystallization) of a chiral analyte is required (perhaps for regulatory purposes) our method should be applicable. It is also possible to perform in situ NMR monitoring of variation of e.e. without using a chiral probe, as a chiral probe might bias the outcome of, for instance, enantiomer enrichment processes[50–52]. Additionally, when a particular analyte is examined using conventional CSA, there exist a set of CSA suitable for each type of analyte (for example, analyte-CSA: carboxylic acids—chiral amines, aminoalcohols—carboxylic acids). Pro-CSA $\mathbf{H}$ based on N,N′-disubstituted oxoporphyrinogen is very versatile in this respect as it provides reasonable chemical shift non-equivalence for a great variety of analytes of different functionality. Another significant feature is that chiral information is first translated from analyte to $\mathbf{H}$ and then read out from $\mathbf{H}$ (in contrast to conventional CSAs) and, as $\mathbf{H}$ operates by hydrogen bonding of the analyte, it can be used to analyse many differently functionalized compounds. As a result of this, $\mathbf{H}$ has four sets of CH reporter groups, which can be varied synthetically (for example, to C-F groups) so that chiral information can be retrieved from ^{19}F NMR spectra where other resonances due to analyte and solvent are absent. Finally, this system is also of note from the point-of-view that it does not rely on the formation of diastereomers. This is perhaps counterintuitive given the prevailing opinion that formation of diastereomers is required in the analysis of e.e.

In summary, a symmetrical a-/prochiral macrocyclic N,N′-disubstituted oxoporphyrinogen host molecule can be utilized as a detector of enantiomeric purity for a wide variety of guest molecules. We have shown that no diastereomeric species are present in solution as complexes with each enantiomer have identical properties. The mechanism of chiral sensing can be rationalized in terms of the host's symmetry and its breakdown when individual host molecule interacts with chiral guest under a fast exchange regime. Chirality sensing (that is, identification of the major enantiomorph) can be achieved by addition of a portion of known enantiomer guest. When a symmetrical molecule is adapted as an e.e. sensor it has certain intrinsic advantages such as identical binding constants for each enantiomer resulting in e.e. determination, which is not obscured by kinetic resolution. The results presented here indicate that other symmetrical molecules should also be available as detectors of enantiopurity using NMR spectroscopy. Such systems might

also improve our understanding of important chirality principles such as majority rule, chirality transfer between molecules and asymmetric reactions.

Methods

Materials. Chloroform-d (Cambridge Isotope Ltd.) for ^{1}H NMR spectroscopy was mostly used as received. In some specific titrations residual water was removed using 4 Å molecular sieves (Wako Chem. Co.). Before use molecular sieves were activated at 200 °C in vacuum. (R)-ibuprofen (Nacalai Tesque), (S)-ibuprofen (TCI Co. Ltd.), (rac)-ibuprofen (TCI Co. Ltd.), (R)-2-phenylpro-pionic acid (Wako Chem. Co.), (rac)-2-phenylpropionic acid (TCI Co. Ltd.), N-boc-L-2-phenylglycine (TCI Co. Ltd.), N-boc-D-2-phenylglycine (TCI Co. Ltd.), N-boc-L-phenylalanine (TCI Co. Ltd.), N-boc-D-phenylalanine (TCI Co. Ltd.), L-leucic acid (TCI Co. Ltd.), DL-leucic acid (TCI Co. Ltd.), (−)-hyoscyamine (TCI Co. Ltd.), (±)-hyoscyamine (TCI Co. Ltd.), (+)-menthol (Sigma-Aldrich Co. LLC.), (−)-menthol (Wako Chem. Co.), (+)-camphor (TCI Co. Ltd.), (−)-camphor (Wako Chem. Co.) were used as received.

Synthesis. (R)-2-phenoxypropionic acid methyl ester and (S)-2-phenoxypropionic acid methyl ester were synthesized from (R)-2-phenoxypropionic acid and (S)-2-phenoxypropionic acid (both Wako Chem. Co.), respectively, through esterification of the corresponding carboxylic acids. 2-Phenoxypropionic acid (1.0 g), iodo-methane (5 equiv.) and potassium carbonate (10 equiv.) were stirred in refluxing acetone (100 ml) for 2 h then acetone was removed under reduced pressure. Crude product was passed through a silica gel column (eluent: dichloromethane, DCM) to yield the final product as a colourless liquid.

D-valine methyl ester and L-valine methyl ester were synthesized from D-valine methyl ester hydrochloride and L-valine methyl ester hydrochloride (both TCI Co. Ltd.), respectively, through neutralization of the corresponding hydrochloride salts. The hydrochloride salt was dissolved in pure water and neutralized using an excess of potassium carbonate solution (pH = c.a. 12) then the aqueous solution was extracted three times using DCM. DCM fractions were combined then dried over anhydrous sodium sulphate. Subsequent filtration and removal of DCM under reduced pressure yielded the final product as a white solid.

Synthesis of host molecule N$_{21}$,N$_{23}$-bis(4-bromobenzyl)-5,10,15,20-$tetrakis$(3,5-di-t-butyl-4-oxocyclohexadien-2,5-ylidene)porphyrinogen (**H**) has been reported previously[53,54].

General spectroscopic methods. ^{1}H NMR spectra were obtained at 25 °C (unless stated otherwise) using an AL300BX spectrometer (JEOL) operating at 300.4 MHz. When variable temperature measurements (VT-^{1}H NMR) were performed the appropriate JEOL temperature control unit (temperature fluctuation ± 0.3 °C) was used. Before the experiment, host **H** was dissolved in chloroform-d (usually ca. 0.6 mM) in an NMR tube and subsequently ligand (chiral guest or water) was added/injected directly into the NMR tube. Molar ratio of ligand and host was carefully determined by integration of the corresponding peaks in spectra. All spectra were referenced to tetramethylsilane. Numbers of scans typically used (for ca. 0.6 mM of host molecule **H**): 16–32 scans for samples up to 500 equiv. of guest **G***; 32–128 scans for samples containing from 500–1,000 equiv. of **G***; 128–512 scans for samples containing in excess of 1,000 equiv. **G***.

Electronic absorption spectra and CD spectra were measured using a J-820 CD spectrophotometer (JASCO) at room temperature (ca. 25 °C). When titration experiments were performed a chloroform-d solution of host **H** (ca. 7×10^{-5} M) was prepared and 0.17 ml of this solution was placed in a 1-mm pathlength quartz cell. In order to maintain host concentration constant chloroform-d stock solutions of host **H** with various chiral guests were prepared ([**H**]$_t$ ca. 7×10^{-5} M, [**G***]$_t$ up to ca. 1.5 M, subscript 't' denotes total concentration) and subsequently titrated into the host solution by using a syringe (0–600 μl). Then uv/Vis and CD spectra were recorded simultaneously.

Derivation of competitive binding model. From equilibrium equations 1, the equilibrium binding constants and mass balance equations can then be expressed as equations 4.

$$K_{HG^*} = \frac{[HG^*]}{[H][G^*]}$$
$$K_{HW} = \frac{[HW]}{[H][W]}$$
$$[G^*]_t = [G^*] + [HG^*]$$
$$[W]_t = [W] + [HW]$$
$$[H]_t = [H] + [HG^*] + [HW]$$
(4)

where [**H**]$_t$, [**G***]$_t$ and [**W**]$_t$ denote total concentrations of **H**, **G*** and **W**, respectively. [H], [**G***] and [W] denote concentrations of free **H**, **G*** and **W**, respectively. [HG*] and [HW] are concentrations of the corresponding complexed forms. A solution (especially values of [HG*], [H] and [HW]) can be obtained using either numerical Newton iterative methods or rather complex but exact analytic solution

(see Supplementary Methods). Then populations of all the host forms (one free and two bound) can be expressed in the form of equations 5.

$$p_{HG^*} = \frac{[HG^*]}{[H]_t}, \ p_H = \frac{[H]}{[H]_t}, \ p_{HW} = \frac{[HW]}{[H]_t}$$
(5)

Because of fast exchange between the three states of host **H**·**G***, **H** and **H**·**W** (Fig. 5a) the resulting chemical shift of pyrrolic NH, δ_{NH}, takes the form of a population averaged chemical shift of the respective states (Fig. 5b) and can be expressed as equation 2.

Similarly, a $\Delta\delta$ binding isotherm (describing chemical shift non-equivalence) can be constructed under the following assumptions. For reasons of symmetry, we assume that the binding of (R)- or (S)-enantiomers to the host is statistical. When a chiral guest **G*** binds to the host the probability that the site is occupied by (R)- or (S)-enantiomer can be determined as a function of e.e. by equations 6.

$$p_R(e.e.) = \frac{[G_R]_t}{[G_R]_t + [G_S]_t} = \frac{1 + e.e.}{2}, \ p_S(e.e.) = \frac{[G_S]_t}{[G_R]_t + [G_S]_t} = \frac{1 - e.e.}{2}$$
(6)

where [G_R]$_t$ and [G_S]$_t$ are total concentrations of (R)- and (S)-enantiomer, respectively. As mentioned above, the ^{1}H–^{1}H COSY spectrum of the pyrrolic β-H resonance indicates that both split peaks must be at the same pyrrolic ring. Moreover, mirror symmetry of the host's binding site and the intrinsic saddle shape of the host's macrocycle causes a preference for certain mutual host–guest conformations (see MD study, Fig. 2c,d) and therefore does not permit isotropic rotation of guest at the binding site. Thus, when chiral guest is present, an asymmetric shielding effect at (for example) pyrrolic β-H positions occurs. In this situation, the chemical shift of respective pyrrolic β-H is given by equations 7.

$$^\beta\delta_{HG^*,A} = {}^\beta\delta_{A,R} \ p_R(e.e.) + {}^\beta\delta_{A,S} \ p_S(e.e.)$$
(7)

$$^\beta\delta_{HG^*,B} = {}^\beta\delta_{B,R} \ p_R(e.e.) + {}^\beta\delta_{B,S} \ p_S(e.e.)$$

where $^\beta\delta_{HG^*,A}$ and $^\beta\delta_{HG^*,B}$ are chemical shifts of protons H$_A$ and H$_B$ (for labels see Fig. 5), respectively, when only chiral guests under fast exchange are considered to bind to the host molecule (Fig. 5c). $^\beta\delta_{A,R}$ and $^\beta\delta_{A,S}$ are chemical shifts of H$_A$ resulting from complexation with neat (R)- and (S)-enantiomers, respectively. $^\beta\delta_{B,R}$ and $^\beta\delta_{B,S}$ represent the same quantity for H$_B$. $^\beta\delta_{A,R}$, $^\beta\delta_{A,S}$, $^\beta\delta_{B,R}$ and $^\beta\delta_{B,S}$ are constants for each specific combination of host and chiral guest (at given temperature). Symmetry and chemical shift equivalency between complexes with only (R)- and only (S)-enantiomer implies that $^\beta\delta_{A,R} = {}^\beta\delta_{B,S}$ and $^\beta\delta_{A,S} = {}^\beta\delta_{B,R}$. For convenience let us introduce $\Delta\delta_{max} = {}^\beta\delta_{A,R} - {}^\beta\delta_{B,R}$ as a measure of the maximum chemical shift difference between H$_A$ and H$_B$ protons as a characteristic value for each host–guest combination. When the competitive exchange of **G*** with water **W** is taken into account the overall chemical shift $^\beta\delta_A$ and $^\beta\delta_B$ of protons H$_A$ and H$_B$, respectively, will be described as population weighted chemical shifts (Fig. 5c) of respective types of host by equations 8.

$$^\beta\delta_A = p_{HG^*} \times {}^\beta\delta_{HG^*,A} + p_H \times {}^\beta\delta_H + p_{HW} \times {}^\beta\delta_{HW}$$
(8)

$$^\beta\delta_B = p_{HG^*} \times {}^\beta\delta_{HG^*,B} + p_H \times {}^\beta\delta_H + p_{HW} \times {}^\beta\delta_{HW}$$

where $^\beta\delta_H$ and $^\beta\delta_{HW}$ are chemical shifts of N-alkylated pyrrolic β-H corresponding to free host **H** and host complexed to water **H**·**W**, respectively. $^\beta\delta_H$ and $^\beta\delta_{HW}$ have the same values for H$_A$ and H$_B$ protons as there is no induced asymmetry here. Hence, under the above assumptions, the binding isotherm for the chemical shift difference $\Delta\delta = {}^\beta\delta_A - {}^\beta\delta_B$ for the N-alkylated pyrrolic β-H will have the form of equation 3. The same derivation of binding isotherm applied to N-H pyrrolic β-H also applies to hemiquinonoid $ortho$-H resonances in case of guest **4**.

References

1. Hutt, A. J. in *Introduction to the Principles of Drug Design and Action* (ed. Smith, H. J.) Chapter 5 (CRC Press, Taylor & Francis, 2006).
2. *Comprehensive organic catalysis, Vols I to III* (eds Jacobsen, E. N., Pfaltz, A. & Yamamoto, H.) (Springer, 1999).
3. Heitbaum, M., Glorius, F. & Escher, I. Asymmetric heterogeneous catalysis. *Angew. Chem. Int. Ed.* **45,** 4732–4762 (2006).
4. Yoon, T. P. & Jacobsen, E. N. Privileged chiral catalysts. *Science* **299,** 1691–1693 (2003).
5. Kondo, T., Oyama, K. & Yoshida, K. Chiral molecular recognition on formation of a metalloanthocyanin: a supramolecular metal complex pigment from blue flowers of Salvia patens. *Angew. Chem. Int. Ed* **40,** 894–897 (2001).
6. Ishi-i, T., Crego-Calama, M., Timmerman, P., Reinhoudt, D. N. & Shinkai, S. Enantioselective formation of a dynamic hydrogen-bonded assembly based on the chiral memory concept. *J. Am. Chem. Soc.* **124,** 14631–14641 (2002).
7. Maeda, K., Morino, K., Okamoto, Y., Sato, T. & Yashima, E. Mechanism of helix induction on a stereoregular poly((4-carboxyphenyl)acetylene) with chiral amines and memory of the macromolecular helicity assisted by interaction with achiral amines. *J. Am. Chem. Soc.* **126,** 4329–4342 (2004).
8. Scarso, A., Shivanyuk, A., Hayashida, O. & Rebek, J., Jr. Asymmetric environments in encapsulation complexes. *J. Am. Chem. Soc.* **125,** 6239–6243 (2003).

9. Yu, J., RajanBabu, T. V. & Parquette, J. R. Conformationally driven asymmetric induction of a catalytic dendrimer. *J. Am. Chem. Soc.* **130**, 7845–7847 (2008).

10. Hirschberg, J. H. K. K. *et al.* Helical self-assembled polymers from cooperative stacking of hydrogen-bonded pairs. *Nature* **407**, 167–170 (2000).

11. Kubo, Y., Maeda, S., Tokita, S. & Kubo, M. Colorimetric chiral recognition by a molecular sensor. *Nature* **382**, 522–524 (1996).

12. Zhu, L. & Anslyn, E. V. Facile quantification of enantiomeric excess and concentration with indicator-displacement assays: an example in the analyses of α-hydroxyacids. *J. Am. Chem. Soc.* **126**, 3676–3677 (2004).

13. Tsubaki, K. *et al.* Visual enantiomeric recognition using chiral phenolphthalein derivatives. *Org. Lett.* **3**, 4071–4073 (2001).

14. Mizuno, Y., Aida, T. & Yamaguchi, K. Chirality-memory molecule: crystallographic and spectroscopic studies on dynamic molecular recognition events by fully substituted chiral porphyrins. *J. Am. Chem. Soc.* **122**, 5278–5285 (2000).

15. Nieto, S., Lynch, V. M., Anslyn, E. V., Kim, H. & Chin, J. High-throughput screening of identity, enantiomeric excess, and concentration using MLCT transitions in CD spectroscopy. *J. Am. Chem. Soc.* **130**, 9232–9233 (2008).

16. James, T. D., Sandanayake, K. R. A. S. & Shinkai, S. Chiral discrimination of monosaccharides using a fluorescent molecular sensor. *Nature* **374**, 345–347 (1995).

17. Matsushita, M. *et al.* High-throughput screening by using a blue-fluorescent antibody sensor. *Angew. Chem. Int. Ed* **42**, 5984–5987 (2003).

18. Mei, X. & Wolf, C. Enantioselective sensing of chiral carboxylic acids. *J. Am. Chem. Soc.* **126**, 14736–14737 (2004).

19. Yu, S. & Pu, L. Pseudoenantiomeric fluorescent sensors in a chiral assay. *J. Am. Chem. Soc.* **132**, 17698–17700 (2010).

20. Mirri, G. *et al.* Electrochemical method for the determination of enantiomeric excess of binol using redox-active boronic acids as chiral sensors. *J. Am. Chem. Soc.* **132**, 8903–8905 (2010).

21. Rekharsky, M. V. *et al.* Chiral recognition in cucurbituril cavities. *J. Am. Chem. Soc.* **128**, 14871–14880 (2006).

22. Borovkov, V. V., Lintuluoto, J. M. & Inoue, Y. Supramolecular chirogenesis in zinc porphyrins: mechanism, role of guest structure, and application for the absolute configuration determination. *J. Am. Chem. Soc.* **123**, 2979–2989 (2001).

23. Kubo, Y. *et al.* Chirality-transfer control using a heterotopic zinc(II) porphyrin dimer. *J. Am. Chem. Soc.* **123**, 12700–12701 (2001).

24. Li, X., Tanasova, M., Vasileiou, C. & Borhan, B. Fluorinated porphyrin tweezer: a powerful reporter of absolute configuration for *erythro* and *threo* diols, amino alcohols, and diamines. *J. Am. Chem. Soc.* **130**, 1885–1893 (2008).

25. Huang, X. Absolute configurational assignments of secondary amines by CD-sensitive dimeric zinc porphyrin host. *J. Am. Chem. Soc.* **124**, 10320–10335 (2002).

26. Dale, J. A., Dull, D. L. & Mosher, H. S. α-Methoxy-α-trifluoromethylphenylacetic acid, a versatile reagent for the determination of enantiomeric composition of alcohols and amines. *J. Org. Chem.* **34**, 2543–2549 (1969).

27. Parker, D. NMR determination of enantiomeric purity. *Chem. Rev.* **91**, 1441–1457 (1991).

28. Wenzel, T. J. & Chisholm, C. D. Assignment of absolute configuration using chiral reagents and NMR spectroscopy. *Chirality* **23**, 190–214 (2011).

29. Duddeck, H. & Gómez, E. D. Chiral recognition of ethers by NMR spectroscopy. *Chirality* **21**, 51–68 (2009).

30. Schwenninger, R. *et al.* Metal complexes of a biconcave porphyrin with *D*₄-structure - versatile chiral shift agents. *Chem. Eur. J.* **7**, 2676–2686 (2001).

31. Williams, T., Pitcher, R. G., Bommer, P., Gutzwiller, J. & Uskoković, M. Diastereomeric solute-solute interactions of enantiomers in achiral solvents. Nonequivalence of the nuclear magnetic resonance spectra of racemic and optically active dihydroquinine. *J. Am. Chem. Soc.* **91**, 1871–1872 (1969).

32. Dobashi, A., Saito, N., Motoyama, Y. & Hara, S. Self-induced nonequivalence in the association of D and L-amino acid derivatives. *J. Am. Chem. Soc.* **108**, 307–308 (1986).

33. Luchinat, C. & Roelens, S. Enantiomeric purity determination of 1,2-diols through NMR spectroscopy without chiral auxiliaries. *J. Am. Chem. Soc.* **108**, 4873–4878 (1986).

34. Feringa, B. L., Smaardijk, A. & Wynberg, H. Simple ³¹P NMR method for the determination of enantiomeric purity of alcohols not requiring chiral auxiliary compounds. *J. Am. Chem. Soc.* **107**, 4798–4799 (1985).

35. Shundo, A., Labuta, J., Hill, J. P., Ishihara, S. & Ariga, K. Nuclear magnetic resonance signaling of molecular chiral information using an achiral reagent. *J. Am. Chem. Soc.* **131**, 9494–9495 (2009).

36. Labuta, J. *et al.* Chirality sensing by nonchiral porphines. *Chem. Eur. J.* **17**, 3558–3561 (2011).

37. Merlet, D., Loewenstein, A., Smadja, W., Courtieu, J. & Lesot, P. Quantitative description of the facial discrimination of molecules containing a prochiral group by NMR in a chiral liquid crystal. *J. Am. Chem. Soc.* **120**, 963–969 (1998).

38. Merlet, D., Emsley, J. W., Lesot, P. & Courtieu, J. The relationship between molecular symmetry and second-rank orientational order parameters for molecules in chiral liquid crystalline solvents. *J. Chem. Phys.* **111**, 6890–6896 (1999).

39. Aroulanda, C., Merlet, D., Courtieu, J. & Lesot, P. NMR experimental evidence of the differentiation of enantiotopic directions in *C*ₛ and *C*₂ᵥ molecules using partially oriented, chiral media. *J. Am. Chem. Soc.* **123**, 12059–12066 (2001).

40. Guijarro, A. & Yus, M. *The Origin of Chirality in the Molecules of Life* (RSC Publishing, 2009).

41. Hanson, K. R. Applications of the sequence rule. I. Naming the paired ligands g,g at a tetrahedral atom xggij. II. Naming the two faces of a trigonal atom yghi. *J. Am. Chem. Soc.* **88**, 2731–2742 (1966).

42. IUPAC Gold Book: http://goldbook.iupac.org/P04859.html (2012).

43. Fulwood, R. & Parker, D. 1,2-diphenylethane-1,2-diamine: An effective NMR chiral solvating agent for chiral carboxylic acids. *J. Chem. Soc., Perkin Trans. 2* 57–64 (1994).

44. Eliel, E. L. Prostereoisomerism (Prochirality). *Top. Curr. Chem.* **105**, 1–76 (1982).

45. Mislow, K. & Siege, J. Stereoisomerism and local chirality. *J. Am. Chem. Soc.* **106**, 3319–3328 (1984).

46. Anslyn, E. V. & Dougherty, D. A. *Modern Physical Organic Chemistry* 315–316 (University Science Books, 2005).

47. Ishihara, S. *et al.* Colorimetric detection of trace water in tetrahydrofuran using N,N'-substituted oxoporphyrinogens. *Chem. Commun.* **48**, 3933–3935 (2012).

48. Ingham, K. C. On the application of Job's method of continuous variation to the stoichiometry of protein-ligand complexes. *Anal. Biochem.* **68**, 660–663 (1975).

49. Soai, K., Shibata, T., Morioka, H. & Choji, K. Asymmetric autocatalysis and amplification of enantiomeric excess of a chiral molecule. *Nature* **378**, 767–768 (1995).

50. Klussmann, M. *et al.* Thermodynamic control of asymmetric amplification in amino acid catalysis. *Nature* **441**, 621–623 (2006).

51. Perry, R. H., Wu, C., Nefliu, M. & Cooks, R. G. Serine sublimes with spontaneous chiral amplification. *Chem. Commun.* 1071–1073 (2007).

52. Fletcher, S. P., Jagt, R. B. C. & Feringa, B. L. An astrophysically-relevant mechanism for amino acid enantiomer enrichment. *Chem. Commun.* 2578–2580 (2007).

53. Hill, J. P., Schmitt, W., McCarty, A. L., Ariga, K. & D'Souza, F. Structures, spectral and electrochemical properties of N-(naphth-2-ylmethyl)-appended porphyrinogens. *Eur. J. Org. Chem.* 2893–2902 (2005).

54. Hill, J. P. *et al.* Highly nonplanar, electron deficient, N-substituted tetra-oxocyclohexadienylidene porphyrinogens: structural, computational, and electrochemical investigations. *J. Org. Chem.* **69**, 5861–5869 (2004).

Acknowledgements

Author contributions

J.L. and S.I. developed the concept of a non-diastereomeric sensing mechanism assisted by A.S. J.L. and S.I. designed and performed experiments and data analysis. J.L. processed/fitted experimental data using mathematical models. S.I. synthesized several of the guest molecules. T.S., L.H. and J.V.B. performed QM calculations. Z.F. performed MD simulations. K.A. discussed results and proposed experiments. J.P.H. prepared and purified the host molecule. J.L. and J.P.H. directed the research and wrote the manuscript with input from all other authors.

Additional information